AMERICAN SOCIETY FOR MICROBIOLOGY | Journal of Virology

Residues K465 and G467 within the Cytoplasmic Domain of GP2 Play a Critical Role in the Persistence of Lymphocytic Choriomeningitis Virus in Mice

Masaharu Iwasaki, Cherie T. Ng, Beatrice Cubitt, Juan C. de la Torre

Department of Immunology and Microbial Science, Scripps Research Institute, La Jolla, California, USA

ABSTRACT

Several arenaviruses, chiefly Lassa virus (LASV), cause hemorrhagic fever disease in humans and pose serious public health concerns in their regions of endemicity. Moreover, mounting evidence indicates that the worldwide-distributed prototypic arenavirus, lymphocytic choriomeningitis virus (LCMV), is a neglected human pathogen of clinical significance. We have documented that a recombinant LCMV containing the glycoprotein (GPC) gene of LASV within the backbone of the immunosuppressive clone 13 (Cl-13) variant of the Armstrong strain of LCMV (rCl-13/LASV-GPC) exhibited Cl-13-like growth properties in cultured cells, but in contrast to Cl-13, rCl-13/LASV-GPC was unable to establish persistence in immunocompetent adult mice, which prevented its use for some *in vivo* experiments. Recently, V459K and K461G mutations within the GP2 cytoplasmic domain (CD) of rCl-13/LASV-GPC were shown to increase rCl-13/LASV-GPC infectivity in mice. Here, we generated rCl-13(GPC/VGKS) by introducing the corresponding revertant mutations K465V and G467K within GP2 of rCl-13 and we show that rCl-13(GPC/VGKS) was unable to persist in mice. K465V and G467K mutations did not affect GPC processing, virus RNA replication, or gene expression. In addition, rCl-13(GPC/VGKS) grew to high titers in cultured cell lines and in immunodeficient mice. Further analysis revealed that rCl-13(GPC/VGKS) infected fewer splenic plasmacytoid dendritic cells than rCl-13, yet the two viruses induced similar type I interferon responses in mice. Our findings have identified novel viral determinants of Cl-13 persistence and also revealed that virus GPC-host interactions yet to be elucidated critically contribute to Cl-13 persistence.

IMPORTANCE

The prototypic arenavirus, lymphocytic choriomeningitis virus (LCMV), provides investigators with a superb experimental model system to investigate virus-host interactions. The Armstrong strain (ARM) of LCMV causes an acute infection, whereas its derivative, clone 13 (Cl-13), causes a persistent infection. Mutations F260L and K1079Q within GP1 and L polymerase, respectively, have been shown to play critical roles in Cl-13's ability to persist in mice. However, there is an overall lack of knowledge about other viral determinants required for Cl-13's persistence. Here, we report that mutations K465V and G467K within the cytoplasmic domain of Cl-13 GP2 resulted in a virus, rCl-13(GPC/VGKS), that failed to persist in mice despite exhibiting Cl-13 wild-type-like fitness in cultured cells and immunocompromised mice. This finding has uncovered novel viral determinants of viral persistence, and a detailed characterization of rCl-13(GPC/VGKS) can provide novel insights into the mechanisms underlying persistent viral infection.

Arenaviruses are enveloped viruses with a bisegmented negative-strand RNA genome (1). Each genome segment, L and S, uses an ambisense coding strategy to direct the synthesis of two proteins in opposite orientations, separated by a noncoding intergenic region (IGR) (1). The S RNA encodes the viral nucleoprotein (NP) and the glycoprotein precursor (GPC), which is cotranslationally cleaved by the signal peptidase to generate a 58-amino-acid stable signal peptide (SSP) and posttranslationally processed by the site 1 protease (S1P) to generate the mature virion surface glycoproteins GP1 and GP2 that, together with SSP, form the GP complex that mediates virus receptor recognition and cell entry. The L RNA encodes the viral RNA-dependent RNA polymerase (L) and the matrix RING finger protein Z (2, 3).

Several arenaviruses cause hemorrhagic fever (HF) disease in humans and pose important public health problems within their regions of endemicity (1, 4, 5). Lassa virus (LASV) is the arenavirus with the greatest impact on human health. LASV infects several hundred thousand individuals yearly in West Africa, resulting in a high number of Lassa fever (LF) cases associated with high morbidity and significant mortality (6). Notably, increased travel has led to the importation of LF cases into metropolitan areas of nonendemicity around the globe (7, 8). Moreover, LASV regions of endemicity are expanding (6), and the association of the recently identified arenavirus Lujo virus with a recent outbreak of HF in South Africa (9, 10) has raised concerns about the emergence of novel HF arenaviruses. Concerns about human-pathogenic arenaviruses are exacerbated because there are no FDA-licensed arenavirus vaccines (11) and current antiarenaviral therapy is limited to off-

Received 1 July 2016 **Accepted** 22 August 2016

Accepted manuscript posted online 31 August 2016

Citation Iwasaki M, Ng CT, Cubitt B, de la Torre JC. 2016. Residues K465 and G467 within the cytoplasmic domain of GP2 play a critical role in the persistence of lymphocytic choriomeningitis virus in mice. J Virol 90:10102–10112. doi:10.1128/JVI.01303-16.

Editor: D. S. Lyles, Wake Forest University

Address correspondence to Juan C. de la Torre, juanct@scripps.edu.

This is article number 29363 from The Scripps Research Institute.

label use of ribavirin that is only partially effective (12–14). Evidence indicates that morbidity and mortality associated with LASV, as well as other HF arenaviruses, involves a failure of the host's innate immune response to restrict virus replication and to facilitate the initiation of an effective adaptive immune response (15). Hence, the development of novel strategies to combat HF arenaviruses will benefit from the identification and functional characterization of viral factors that contribute to virus escape from control by the host defenses at early times of infection.

Intravenous (i.v.) inoculation of adult immunocompetent mice with a high dose of the Armstrong (ARM) strain of lymphocytic choriomeningitis virus (LCMV) results in an acute infection that is cleared within 10 to 14 days by a robust protective immune response mediated mainly by virus-specific $CD8^+$ cytotoxic T lymphocytes (CTLs) (16), whereas infection with the immunosuppressive strain of LCMV, clone 13 (Cl-13), causes persistent infection associated with generalized immune suppression. ARM and Cl-13 differ at only three amino acid positions, two within GP1 (N176D and F260L) and one within the L polymerase (K1079Q) (17, 18). Mutation N176D in GPC was shown to be dispensable for the persistent phenotype of Cl-13, whereas mutations F260L in GPC and K1079Q in L have been shown to increase the virus's ability to infect specific populations of dendritic cells (DCs), which has been implicated in Cl-13 persistence by increasing the expression levels of negative immune-regulatory molecules, including programmed death 1 (PD-1) (19), while interfering with the expression of immune-stimulatory molecules known to contribute to control of chronic viral infection (20–22). Specifically, mutation F260L in GP1 is correlated with a change from low (ARM; F260) to high (Cl-13; L260) affinity for alpha-dystroglycan (αDG), a cell surface receptor present at high levels in DCs and used by several arenaviruses, including Cl-13 and LASV, as the primary cell entry receptor (18, 23, 24). However, little is known about other viral factors that may contribute to Cl-13's ability to persist in mice.

A recombinant Cl-13 in which LASV-GPC substituted for the Cl-13 GPC gene (rCl-13/LASV-GPC) grew to high titer in cultured cells but was unable to establish persistence in adult C57BL/6J (B6) mice (25). However, a point mutation, K461G, within GP2 that emerged during replication of rCl-13/LASV-GPC in a mouse resulted in a mutant rCl-13/LASV-GPC that persisted for about 2 weeks in adult B6 mice (26). Characterization of additional LCMV/LASV-GPC mutants revealed that the presence of both V459K and K461G mutations within LASV GP2 further increased the virus's ability to replicate in B6 mice (26). These findings led us to investigate whether the counterpart K465 and G467 residues in Cl-13 GP2 played a critical role in Cl-13 persistence. To address this question, we generated a recombinant Cl-13 containing amino acid mutations K465V and G467K in the cytoplasmic domain (CD) of GP2 [rCl-13(GPC/VGKS)] and examined its phenotypic properties, including its ability to establish persistence in immunocompetent adult B6 mice. Here, we show that rCl-13(GPC/VGKS) failed to persist in B6 mice. The K465V and G467K mutations did not significantly affect the biochemical features of GPC or viral fitness in cultured cells and immunocompromised mice. Consistent with its inability to persist in B6 mice, rCl-13(GPC/VGKS) infected a lower number of plasmacytoid dendritic cells (pDCs) in the spleen than the rCl-13 wild type (WT), but rCl-13 WT and rCl-13(GPC/VGKS) induced similar levels of type I interferon (IFN-I) at early times of infection in B6 mice. Our findings indicate that the K465 and G467 residues in the CD of Cl-13 GP2 are critical for the establishment of Cl-13 persistence in immunocompetent adult mice.

MATERIALS AND METHODS

Plasmids. pCAGGS-NP (pC-NP), pCAGGS-L (pC-L), and pCAGGS-GPC Cl-13 (pC-GPC) have been described previously (27–29). pC-GPC/VGKS was generated by PCR-based mutagenesis to incorporate K465V and G467K mutations into the GPC gene of pC-GPC. Plasmids for rescue of rLCMV were generated based on the pPol1S Cl-13 and pPol1L Cl-13 plasmids, which direct RNA polymerase I (Pol1)-mediated intracellular synthesis of S and L, respectively, RNA genome species of the Cl-13 strain of LCMV (30, 31). pPol1S Cl-13(GPC/VGKS) was generated by PCR-based mutagenesis introducing K465V and G467K mutations into the GPC gene of pPol1S Cl-13. pPol1S Cl-13(LASV-GPC/KGGS) was generated by PCR-based mutagenesis introducing V459K and K461G mutations into the LASV GPC gene of a pPol1S Cl-13 construct in which LASV GPC substituted for Cl-13 GPC (25).

Cells. BHK-21, L929, Vero, A549, and 293T cells were grown in Dulbecco's modified Eagle's medium (DMEM) (Invitrogen) containing 10% fetal bovine serum (FBS), 2 mM L-glutamine, 100 μg/ml streptomycin, and 100 U/ml penicillin at 37°C and 5% CO_2.

Generation of rLCMV. The different rLCMVs used in this study were generated as described previously (30–32) with minor modifications. BHK-21 cells seeded at 7.5×10^5 cells/well (6-well plate) were cultured overnight and transfected with plasmids pPol1S (0.8 μg) and pPol1L (1.4 μg), together with plasmids pC-NP (0.8 μg) and pC-L (1.0 μg), using 2.5 μl of Lipofectamine 2000 (LF2000) (Invitrogen)/μg of DNA. After 5 h of transfection, the transfection mixture was removed and fresh medium was added. At 3 days posttranfection, the tissue culture supernatant (TCS) was removed, 3 ml of fresh medium was added, and the cells were cultured for another 3 days. The TCS collected at 6 days posttransfection was designated passage 0 (P0). Rescued viruses were amplified by infection of BHK-21 cells (multiplicity of infection [MOI] = 0.01). At 72 h postinfection (p.i.), TCSs were collected and clarified by centrifugation at $400 \times g$ and 4°C for 5 min to remove cell debris and stored at −80°C. To generate rCl-13(GPC/VGKS) and rCl-13(LASV-GPC/KGGS), pPol1S Cl-13(GPC/VGKS) and pPol1S Cl-13(LASV-GPC/KGGS), respectively, were used, together with pPol1L Cl-13.

Virus titration. LCMV titers were determined using an immunofocus assay, as described previously (33). Briefly, 10-fold serial virus dilutions were used to infect Vero cell monolayers in a 96-well plate, and at 20 h p.i., the cells were fixed with 4% paraformaldehyde (PFA) in phosphate-buffered saline (PBS). After cell permeabilization by treatment with 0.3% Triton X-100 in PBS containing 3% bovine serum albumin (BSA), the cells were stained with a rat monoclonal antibody (MAb) to NP (VL-4; Bio X Cell) conjugated with Alexa Fluor 488 (protein-labeling kit; Life Technologies).

Mice and virus infection *in vivo*. Six-week-old C57BL/6J and IFN-I receptor knockout ($IFNAR^{-/-}$) mice were infected i.v. with rLCMVs (2×10^6 focus-forming units [FFU]) unless otherwise indicated. Blood was collected from the mice under isoflurane anesthesia, and serum was isolated by centrifugation at 12,000 rpm for 3 min. Organs were harvested from euthanized mice and homogenized in DMEM containing 1% FBS. Virus titers in sera and organs were determined by an immunofocus assay. All animal experiments were done under protocol 09-0137 approved by the Scripps Research Institute IACUC.

Western blotting. Total cell lysates were prepared in lysis buffer (1% NP-40, 50 mM Tris-HCl [pH 8.0], 62.5 mM EDTA, 0.4% sodium deoxycholate) and clarified by centrifugation at 15,000 rpm and 4°C for 10 min. The clarified lysates were mixed at a 1:1 ratio with loading buffer (100 mM Tris [pH 6.8], 20% 2-mercaptoethanol, 4% SDS, 0.2% bromophenol blue, 20% glycerol) and boiled for 5 min. Protein samples were fractionated by SDS-polyacrylamide gel electrophoresis (PAGE) using 4 to 20% gradient polyacrylamide gels (Mini-Protein TGX gels; 4 to 20%; Bio-Rad) and

electroblotted onto polyvinylidene difluoride membranes (Immobilon transfer membranes; Millipore). To detect GPC, GP2, and α-tubulin, membranes were reacted with mouse monoclonal antibody to GP2 (We33/36) or rabbit polyclonal antibody to α-tubulin (Cell Signaling Technologies), followed by incubation with horseradish peroxidase-conjugated anti-mouse, or anti-rabbit, respectively, immunoglobulin G (IgG) antibody (Jackson ImmunoResearch Laboratories). SuperSignal West Pico or Femto chemiluminescent substrate (Thermo Scientific) was used to elicit chemiluminescent signals that were visualized using an ImageQuant LAS 4000 Imager (GE Healthcare Life Science).

Northern blotting. Total cellular RNA was isolated using TRI Reagent according to the manufacturer's instructions and analyzed by Northern blotting hybridization. RNA samples were fractionated by 2.2 M formaldehyde-agarose (1.2%) gel electrophoresis, followed by transfer of the RNA in 20× SSC (3 M sodium chloride, 0.3 M sodium citrate) to a Magnagraph membrane using the rapid downward transfer system (TurboBlotter; GE Healthcare Life Sciences). The membrane-bound RNA was cross-linked by exposure to UV light, and the membrane was hybridized to a ^{32}P-labeled GPC-specific antisense riboprobe to detect virus genome RNA and GPC mRNA species.

Virus growth kinetics. Cells were infected with rLCMVs at an MOI of either 0.1 or 0.01, as indicated in the figure legends, and at several times p.i., TCSs were collected and viral titers were determined using an immunofocus assay.

Flow cytometry for detection of splenocytes expressing LCMV NP. Spleens were harvested from mice infected (2×10^6 FFU i.v.) with either rCl-13 WT or rCl-13(GPC/VGKS) for 24 h, incubated with 1 mg/ml collagenase D/100 μg DNase I, and processed into single-cell suspensions through a 70-μm cell strainer (Corning Life Science) before lysing of the erythrocytes with ammonium chloride. The splenocytes were stained with anti-murine antibodies against specific markers for each cell type subset. The following antibodies were used for splenocyte staining: (i) dendritic cells (peridinin chlorophyll protein [PerCP]-Cy5.5 CD11c; allophycocyanin [APC] PDCA-1; BV421 CD8a; phycoerythrin [PE]-Cy7 CD3, CD19, and NK1.1; APC-Cy7 F4/80; and PE SiglecH); (ii) macrophages and monocytes (APC-Cy7 F4/80; PerCP-Cy5.5 Ly6c; Pac Blue Ly6G; APC CD11b; PE CD169; and PE-Cy7 CD3, CD19, and NK1.1); (iii) T, B, and NK cells (e450 CD90, APC-Cy7 CD4, PE-Cy7 CD8, PE CD19, APC CD45, and PerCp-Cy5.5 NK1.1); and (iv) stromal cells (Pac Blue CD45, PAC CD31, PE-Cy7 CD21/CD35, and PE gp38). Intracellular staining for the NP was done by incubating the Alexa Fluor 488-conjugated VL-4 antibody and analyzed by flow cytometry.

Stability of rLCMVs. Cells were seeded 18 h prior to infection with rLCMVs (MOI = 0.01). At 72 h p.i., TCSs were collected and clarified from cell debris by centrifugation at 400 × *g* and 4°C for 5 min, and virus titers were determined by an immunofocus assay. TCS from P1 was used to infect a fresh monolayer of cells, and the same process was repeated over four serial passages. At P4, total RNA was isolated from infected cells and used in reverse transcription (RT)-PCRs to amplify DNA fragments containing GPC, and their sequences were analyzed with Sequencher DNA sequence analysis software (Gene Codes Corporation).

IFN bioassay. L929 cells seeded in 24-well plates at 1.25×10^5 cells/well and cultured overnight were treated with sera (1:100 dilution) from mice infected with rLCMVs (2×10^6 FFU i.v.) collected at 20 h p.i. or infected with rLCMVs (MOI = 0.1). Twenty-four hours later, the cells were infected with recombinant wild-type vesicular stomatitis virus (rVSV) (34) (MOI = 0.01), and at 36 h p.i. with rVSV, the cells were fixed with 4% PFA in PBS and stained with crystal violet.

Detection of apoptotic cells. L929 cells (2.5×10^5 cells/well) seeded in a 12-well plate and cultured overnight were infected with either rCl-13 WT or rCl-13(GPC/VGKS) (MOI = 0.1) for 90 min or remained uninfected (mock infected). At 48 h p.i., cells were collected using Accutase cell detachment solution (Innovative Cell Technologies). For a positive control, mock-infected cells were incubated at 55°C for 20 min. The cells were then stained with fluorescently labeled annexin V according to the manufacturer's instructions (annexin V apoptosis detection kit APC; eBioscience) and fixed with 2% PFA in PBS, and intracellular staining for the NP was done by incubating the Alexa Fluor 488-conjugated VL-4 antibody and analyzed by flow cytometry.

Sensitivity of rLCMVs to exogenous IFN-I. L929 or Vero cells (1.25×10^5 cells/24-well plate) were infected with either rCl-13 WT or rCl-13(GPC/VGKS) (MOI = 0.1) for 90 min and treated with universal IFN-α at a low (5-U/ml) or high (500-U/ml) concentration or remained untreated. At 24 h and 48 h p.i., TCSs were collected, and viral titers were determined using an immunofocus assay.

RESULTS

Generation and characterization of rCl-13 containing mutations K465V and G467K within GP2. LCMV surface glycoproteins are expressed as a single polypeptide, GPC, which is co- and posttranslationally processed into SSP and mature GP1 and GP2 (Fig. 1A). GP2 contains a transmembrane domain (TMD) and a C-terminal CD (Fig. 1B). Residues V459K and K461G within GP2 played a critical role in conferring on rCl-13/LASV-GPC the ability to persist longer in mice (26). To examine whether the corresponding residues were required for Cl-13 persistence, we generated rCl-13(GPC/VGKS), where K465 and G467 were mutated to V and K, respectively, which corresponded to the residues found in LASV GP2 (Fig. 1B). We injected (2×10^6 FFU i.v.) adult C57BL/6J mice with either rCl-13 WT or rCl-13(GPC/VGKS). As expected, rCl-13 WT was able to persist, and viremia was readily detected at 4 and 10 days p.i. (Fig. 1C). In contrast, sera from mice infected with rCl-13(GPC/VGKS) did not contain detectable levels of infectious virus at 4 or 10 days p.i. (Fig. 1C). We examined whether rCl-13(GPC/VGKS) was able to replicate in tissues in the absence of detectable levels of viremia (Fig. 1C). Consistent with previous findings, mice infected with WT Cl-13 contained high levels of infectious virus in the spleen, liver, and kidney at 10 days p.i., whereas we did not detect infectious virus in these tissues in mice infected with rCl-13(GPC/VGKS) (Fig. 1C). These data suggested that K465 and G467 residues are critical for Cl-13 persistence in immunocompetent adult mice.

Effects of K465V and G467K mutations within the CD of GP2 on GPC processing, virus RNA replication, and gene transcription. To investigate possible mechanisms whereby K465V and G467K mutations disrupted Cl-13's ability to persist, we examined whether these mutations affected S1P-mediated processing of GPC, as there is evidence indicating that mutations within the CD of GP2 could influence the efficiency of GPC processing (35, 36). For this, we transfected 293T cells with plasmids expressing either wild-type Cl-13 GPC (GPC WT) or Cl-13 GPC containing K465V and G467K mutations (GPC/VGKS) and assessed GPC processing by Western blotting using an anti-GP2 antibody (Fig. 2A). GPC WT and GPC/VGKS were processed with similar efficiencies. We also examined whether K465V and G467K mutations could interfere with virus RNA replication and gene transcription. For this, we infected BHK-21 cells with either rCl-13 WT or rCl-13(GPC/VGKS) (MOI = 1) and assessed the levels of virus RNA replication and gene transcription by Northern blotting (Fig. 2B). Levels of virus RNA replication and gene transcription were slightly higher in cells infected with rCl-13(GPC/VGKS) than in cells infected with rCl-13 WT at all time points examined, which correlated with slightly (<7.5-fold) higher levels of infectious-virus titers in tissue culture supernatants from cells infected with rCl-13(GPC/VGKS) than in cells infected with rCl-13 WT. These findings suggested that K465V and G467K mutations within the

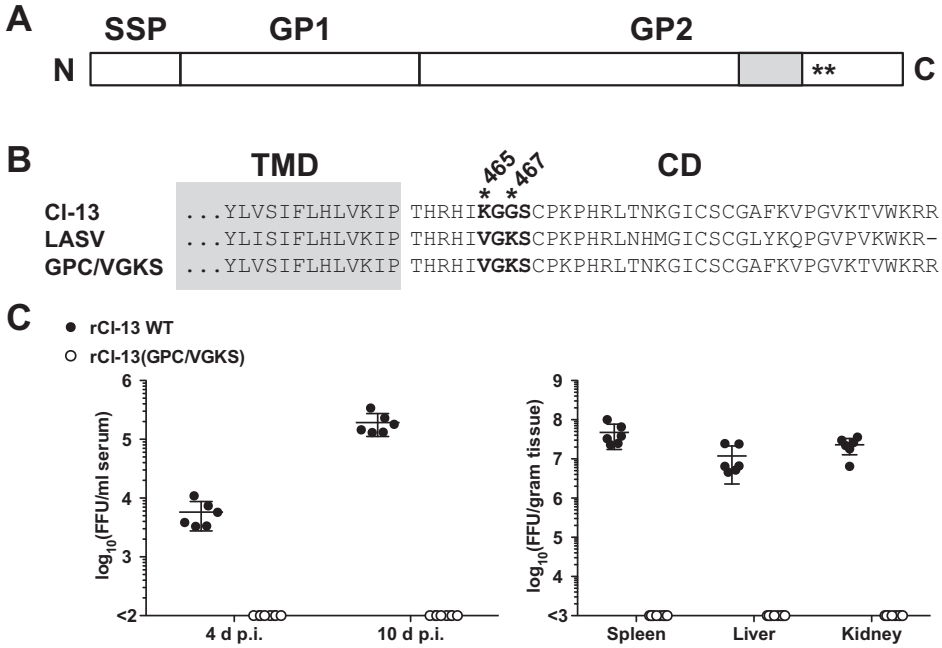

FIG 1 Generation and characterization in mice of rCl-13 containing mutations K465V and G467K within the CD of GP2. (A) Schematic diagram of LCMV GPC. LCMV surface glycoproteins are expressed as a single polypeptide, GPC, which is co- and posttranslationally processed into SSP and the mature GP1 and GP2. The TMD of GP2 is shaded. The asterisks indicate the positions where the mutations were introduced. (B) Amino acid sequence alignment of the C-terminal ends of GP2 from Cl-13, LASV, and Cl-13 containing mutations K465V and G467K (GPC/VGKS). (C) rCl-13(GPC/VGKS) does not persist in adult immunocompetent mice. Six-week-old B6 mice ($n = 6$ per group) were injected (2×10^6 FFU i.v.) with either rCl-13 WT or rCl-13(GPC/VGKS). Blood (4 and 10 days [d] p.i.) and tissues (10 days p.i.), samples were collected from infected mice, and virus titers were determined. The data represent means ± standard deviations (SD) of six mice per group from two independent experiments.

CD of GPC did not negatively impact virus RNA replication and gene transcription.

Effects of K465V and G467K mutations within the CD of Cl-13 GP2 on virus fitness in cultured cells. Next, we asked whether K465V and G467K mutations could affect virus fitness in cultured cells. For this, we examined virus growth kinetics in several types of cell lines, including BHK-21 (a hamster kidney cell line), L929 (a mouse fibroblast line), Vero (an African green monkey kidney cell line), and A549 (a human lung epithelial cell line) cells (Fig. 3A). We observed only modest differences between rCl-13 WT and rCl-13(GPC/VGKS) regarding their growth kinetics and peak titers in BHK-21, A549, and Vero cells. In contrast, in L929 cells, rCl-13(GPC/VGKS) exhibited significantly slower kinetics and a lower peak titer than rCl-13 WT. To gain some initial insights into the genetic stability of rCl-13(GPC/VGKS) in these different cell environments, we conducted serial passages of rCl-13(GPC/VGKS) in each of the cell lines and determined their corresponding GPC sequences from passage 4. Both the K465V and G467K mutations were retained through serial passages in all cell lines tested without evidence of revertant or potential compensatory mutations being present at low frequency. These serial passages of rCl-13(GPC/VGKS) in cultured cells were done using an MOI of 0.1 and infecting 1×10^6 cells each time. Therefore, each infection was initiated with 10^5 infectious particles, which it is highly unlikely to promote exclusion of variants with increased fitness due to bottleneck effects. These findings suggest that the K465V and G467K mutations did not have a major impact on virus fitness in the cell lines tested.

We noticed that in cultured cells rCl-13(GPC/VGKS) showed slower growth kinetics than rCl-13 WT at early times of infection (Fig. 3A). This finding raised the possibility that delayed viral growth at early times of infection was responsible for the failure of rCl-13(GPC/VGKS) to persist in mice, as virus-host interactions at very early times of infection have been shown to dictate whether the host defense responses control and clear the virus or viral persistence takes place (37). However, this is unlikely, because rCl-13(GPC/VGKS) exhibited faster growth kinetics and higher peak titers than rCl-13(LASV-GPC/KGGS), a virus that persisted in mice for about 2 weeks (26) (Fig. 3B).

Effects of K465V and G467K mutations within the CD of GP2 on virus replication in IFN-I-deficient mice. The inability of rCl-13(GPC/VGKS) to persist in mice despite not showing major defects in fitness in cultured cells could have been related to restricted growth of rCl-13(GPC/VGKS) in mice, which would be consistent with our finding that in L929 cells, a mouse fibroblast line, rCl-13(GPC/VGKS) exhibited delayed growth kinetics and lower peak titers than rCl-13 WT. To further investigate this issue, we examined multiplication of rCl-13(GPC/VGKS) in IFN-I-deficient mice. For this, we injected (2×10^6 FFU i.v.) IFNAR$^{-/-}$ mice with either rCl-13 WT or rCl-13(GPC/VGKS). In contrast to infection of WT B6 mice, rCl-13(GPC/VGKS) grew efficiently in IFNAR$^{-/-}$ mice, and viremia was readily detected throughout the experimental period (Fig. 4A). To examine whether K465V and G467K mutations were retained through multiple rounds of infection in mice, we determined the GPC sequences of rCl-13(GPC/VGKS) present in sera at days 4, 10, and 20 p.i. For this, we infected BHK-21 cells with sera from rCl-13(GPC/VGKS)-infected IFNAR$^{-/-}$ mice, and at 72 h p.i., we prepared total cellular

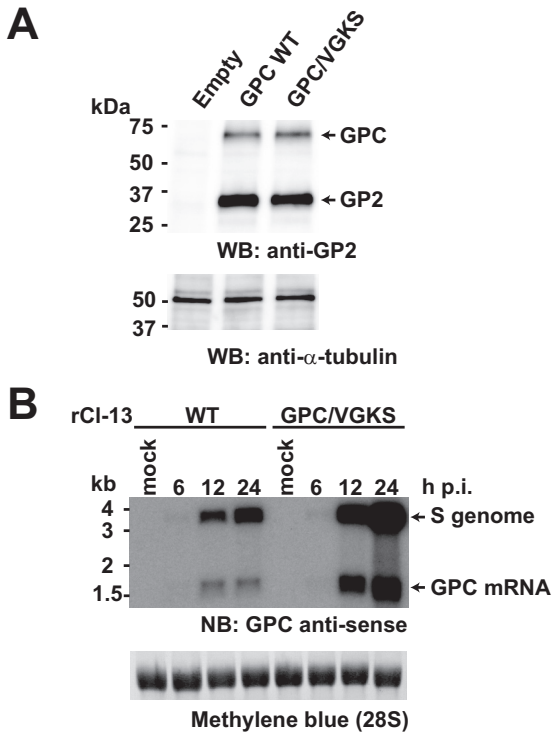

FIG 2 Effects of K465V and G467K mutations on GPC processing and virus RNA replication and gene transcription. (A) Effects of K465V and G467K mutations on GPC processing. 293T cells (3.5×10^5 cells/well) seeded in a 12-well plate were cultured overnight and transfected with 1 μg of pCAGGS-Empty (Empty), pC-GPC Cl-13 (GPC WT), or pC-GPC/VGKS Cl-13 (GPC/VGKS). At 48 h posttransfection, total cell lysates were prepared, and GPC processing was analyzed by Western blotting (WB) using an antibody to GP2. (B) Effects of K465V and G467K mutations on RNA replication and gene transcription. BHK-21 cells (3.5×10^5 cells/well) seeded in a 12-well plate and cultured overnight were infected (MOI = 1.0) with either rCl-13 WT or rCl-13(GPC/VGKS). At the indicated time points, total cellular RNA was isolated and analyzed by Northern blotting (N) using a GPC antisense probe that detected the S genome and GPC mRNA species. 28S rRNA (28S) was detected by methylene blue staining.

RNA that we used to amplify, by RT-PCR, DNA fragments containing the GPC open reading frame (ORF). Sequence analysis revealed that reversion K467G became dominant in one out of five mice at 4 days p.i. (Fig. 4B), and at 10 and 20 days p.i., reversion K467G was detected in all five mice. On the other hand, the K465V mutation was retained in all five mice at all time points examined. These results indicated that rCl-13(GPC/VGKS) can grow to levels similar to those of rCl-13 WT in mice in the absence of the IFN-I system and that G467 has a fitness advantage in mice.

Effects of K465V and G467K mutations on virus tropism at early times of infection in mice. The ability of Cl-13 to infect a larger proportion of pDCs than ARM (20, 38, 39) has been associated with Cl-13's ability to persist in mice, which is due to its higher affinity than ARM for the cell surface receptor αDG (21, 40). Residues K465 and G467 are located within the cytoplasmic domain of GP2, and therefore, it is unlikely that they participate directly in the interaction of rCl-13(GPC/VGKS) with αDG. However, we cannot rule out the possibility that the K465V and G467K mutations could affect, via indirect interactions, the affinity of Cl-13 GP1 for αDG. Alternatively, the K465V and G467K mutations could influence other Cl-13–host interactions that would result in higher numbers of infected pDCs. We therefore examined whether the K465V and G467K mutations affected virus antigen distribution among different immune cell populations in splenocytes isolated from infected mice. For this, we inoculated adult B6 mice (2×10^6 FFU i.v.) with either rCl-13 WT or rCl-13(GPC/VGKS), and 24 h later, we collected spleens and assessed NP-positive (NP^+) cells in different immune cell populations by flow cytometry (Fig. 5A). For all the different immune cell populations examined, with the exception of pDCs, the numbers of NP^+ cells were very similar in rCl-13 WT- and rCl-13(GPC/VGKS)-infected mice. In the case of pDCs, the numbers of NP^+ cells were 2-fold lower in mice infected with rCl-13(GPC/VGKS) than in rCl-13 WT-infected mice. It has been reported that in mice coinfected i.v. with a high dose (2×10^6 PFU each) of Cl-13 (persistent) and ARM (acute), the persistent phenotype of Cl-13 is dominant over the acute phenotype of ARM (16, 37). To examine whether a similar situation was found with rCl-13 WT and rCl-13(GPC/VGKS), we injected (i.v.) adult B6 mice with 2×10^6 FFU of rCl-13 WT, together with 2×10^6 FFU of either rARM WT or rCl-13(GPC/VGKS) (Fig. 5B). Mice coinfected with rCl-13 WT and rCl-13(GPC/VGKS) did not clear the virus and exhibited levels of viremia similar to those of mice coinfected with rCl-13 WT and rARM WT.

Effects of K465V and G467K mutations on virus-mediated induction of IFN-I. IFN-I signaling plays a major role in establishing Cl-13 persistence (39), and differences in the time of onset, magnitude, and duration of virus-mediated induction of IFN-I can significantly influence the outcome of infection (37, 41). We therefore investigated the effects of K465V and G467K mutations on virus-mediated induction of IFN-I in both cultured cells and mice. We first examined whether rCl-13(GPC/VGKS) retained the rCl-13 WT ability to inhibit induction of IFN-I. For this, we infected L929 cells with rCl-13 WT or rCl-13(GPC/VGKS) or, as a control, with mutant rCl-13(NP/D382A), which has been shown to be impaired in its ability to inhibit induction of IFN-I (42). At 24 h p.i. with Cl-13, we infected cells with rVSV WT, and 36 h later, we examined the cells for symptoms of VSV-induced cytopathic effect (CPE) (Fig. 6A). Consistent with previous findings, cells infected with rCl-13(NP/D382A), but not cells infected with rCl-13 WT, were protected against CPE caused by rVSV infection as a result of the cell's antiviral state established by induction of biologically active levels of IFN-I in rCl-13(NP/D382A)-infected cells. In contrast, infection with either rCl-13 WT or rCl-13(GPC/VGKS) did not prevent rVSV-induced CPE, indicating that K465V and G467K mutations within the CD of GP2 did not affect the ability of Cl-13 to prevent induction of IFN-I. These results also indicated that reduced levels of rCl-13(GPC/VGKS), compared to rCl-13 WT, observed in L929 cells (Fig. 3A) were highly unlikely to be related to IFN-I-mediated restriction. Increased levels of apoptosis in rCl-13(GPC/VGKS)-infected L929 cells could also have contributed to reduced levels of virus multiplication. However, L929 cells infected with either rCl-13(GPC/VGKS) or rCl-13 WT displayed only baseline levels of apoptosis, as determined by levels of phosphatidylserine present on the outer leaflet of the plasma membrane detected using fluorescently labeled annexin V (Fig. 6B). Unlike the situation observed in cultured cells, mice infected with Cl-13 exhibit high levels of IFN-I at early times of infection, which has been shown to contribute to establishment of Cl-13 persistence (39). We therefore examined whether rCl-13(GPC/VGKS) and rCl-13 WT induced similar IFN-I responses

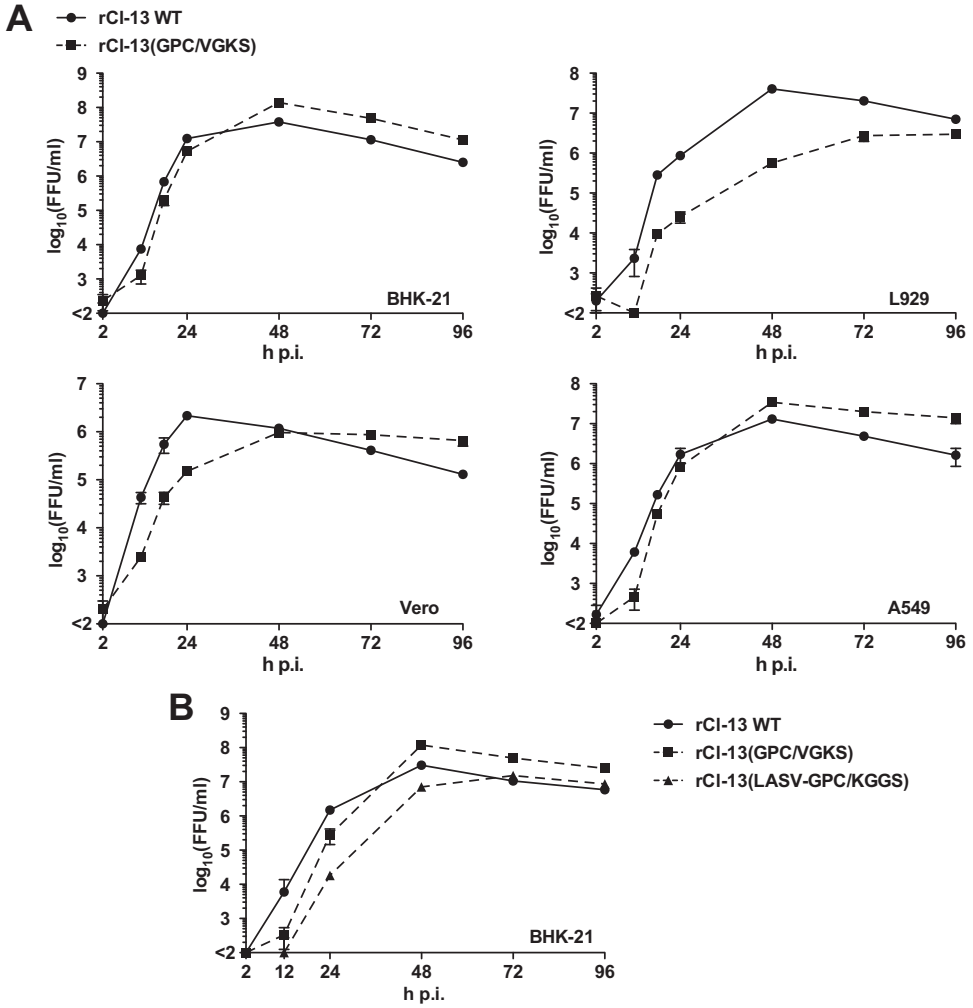

FIG 3 Characterization of rCl-13(GPC/VGKS) growth properties in cultured cells. (A) Growth properties of rCl-13(GPC/VGKS) in different cell lines. L929 (1.25×10^5 cells/well), BHK-21 (1.75×10^5 cells/well), Vero (1.25×10^5 cells/well), or A549 (1.25×10^5 cells/well) cells were seeded in 24-well plates and cultured overnight. The cells were infected (MOI = 0.1) with either rCl-13 WT or rCl-13(GPC/VGKS). At the indicated times, TCSs were collected, and virus titers were determined by an immunofocus assay. The data represent means ± SD of the results of three independent experiments. (B) Comparison of the growth kinetics of rCl-13(GPC/VGKS) and rCl-13(LASV-GPC/KGGS). BHK-21 cells (1.75×10^5 cells/well) were seeded in 24-well plates and cultured overnight, followed by infection (MOI = 0.01) with rCl-13 WT, rCl-13(GPC/VGKS), or rCl-13(LASV-GPC/KGGS). At the indicated times p.i., TCSs were collected and virus titers were determined. The data represent means ± SD of the results of three independent experiments.

in mice. For this, we treated L929 cells with sera (1:100 dilution) prepared from mice at 20 h p.i. (2×10^6 FFU i.v.) with rCl-13 WT, rCl-13(GPC/VGKS), or rCl-13(NP/D382A) or mock-infected (PBS-injected) mice. After 24 h of treatment, we infected the cells with rVSV for 36 h and monitored for the appearance of CPE (Fig. 6C). Treatment with sera from mice infected with either rCl-13 WT or rCl-13(GPC/VGKS), as well as rCl-13(NP/D382A), resulted in the establishment of an effective cell antiviral state reflected in protection against VSV-induced CPE. These data indicated that K465V and G467K mutations affected neither the ability of Cl-13 to inhibit induction of IFN-I in cultured cells nor the IFN-I response in mice following infection (2×10^6 FFU i.v.) with Cl-13. We next asked whether the K465V and G467K mutations could affect the sensitivity of Cl-13 to IFN-I. For this, we infected L929 and Vero cells with either rCl-13 WT or rCl-13(GPC/VGKS) at an MOI of 0.1 for 90 min, followed by treatment with universal IFN-α. At 24 and 48 h p.i., we determined titers of infectious virus in TCS. Although virus titers of rCl-13 WT in L929 TCS were consistently higher than those of rCl-13(GPC/VGKS), rCl-13 WT and rCl-13(GPC/VGKS) showed similar patterns of sensitivity to IFN-α: a low concentration of IFN-α (5 U/ml) reduced virus titers less than 1 log unit at 24 h p.i. and about 1 log unit at 48 h p.i., whereas a high concentration of IFN-α (500 U/ml) reduced virus titers by more than 1 log unit at 24 h p.i. and by more than 3 log units at 48 h p.i. (Fig. 6D). In contrast, and consistent with previous findings (43), rCl-13 WT and rCl-13(GPC/VGKS) were similarly resistant to exogenous IFN-α treatment in Vero cells.

DISCUSSION

Previous work has documented that mutations K1079Q in the L polymerase and F260L in GP1 of ARM resulted in Cl-13's ability to persist in mice. Mutation F260L within GP1 was found to provide Cl-13 with high affinity for αDG (21, 23, 44). This, in turn,

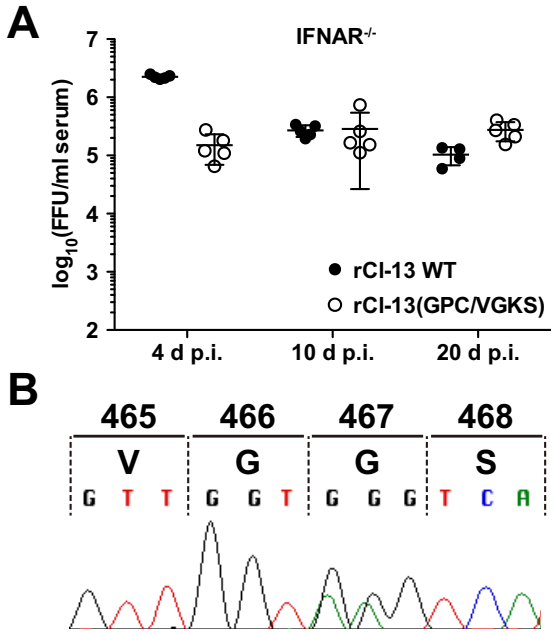

FIG 4 Effects of K465V and G467K mutations on virus replication in mice. (A) rCl-13(GPC/VGKS) persists in IFN-I-deficient mice. IFNAR$^{-/-}$ B6 mice ($n = 5$ per group) were injected (2×10^6 FFU i.v.) with either rCl-13 WT or rCl-13(GPC/VGKS). At the indicated times p.i., blood samples were collected, and serum virus titers were determined by an immunofocus assay. One mouse infected with rCl-13 died at 11 days p.i. The data represent means ± SD among five mice per group. (B) DNA sequence chromatogram of the region containing amino acid positions 465 and 467 of rCl-13(GPC/VGKS) present in serum at 4 days p.i. BHK-21 cells were infected with sera from rCl-13(GPC/VGKS)-infected IFNAR$^{-/-}$ mice. At 72 h p.i., total cellular RNA was isolated from infected cells and used to amplify, by RT-PCR, DNA fragments containing the GPC ORF, and their sequences were analyzed with Sequencher DNA sequence analysis software.

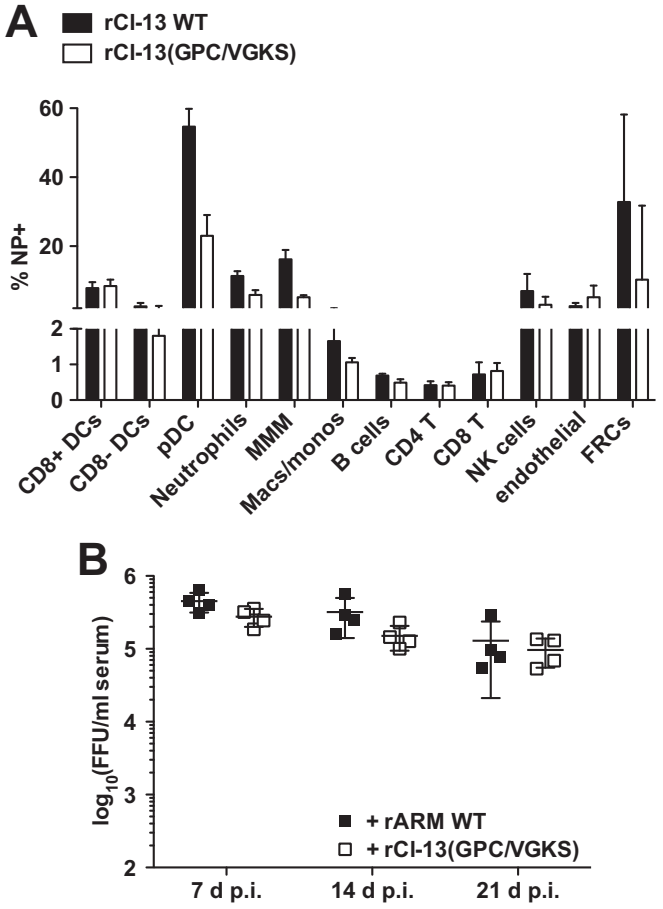

FIG 5 Cell distribution of rCl-13(GPC/VGKS) in spleens of infected mice. (A) Comparison of virus antigen distributions in different immune cell populations in mice infected with either rCl-13 WT or rCl-13(GPC/VGKS). Six-week-old B6 mice ($n = 5$ per group) were injected (2×10^6 FFU i.v.) with either rCl-13 WT or rCl-13(GPC/VGKS). At 24 h p.i., their spleens were collected, and NP-positive cells in different immune cell populations were detected by flow cytometry. The data represent means and SD among five mice per group. MMM, metallophilic marginal zone macrophages; Macs/monos, macrophages and monocytes; NK cells, natural killer cells; FRCs, fibroblastic reticular cells. (B) rCl-13(GPC/VGKS) does not prevent persistence of Cl-13. Six-week-old B6 mice ($n = 4$ per group) were injected (i.v.) with 2×10^6 FFU of either rARM WT or rCl-13(GPC/VGKS), together with 2×10^6 FFU of rCl-13 WT. At the indicated times p.i., blood samples were collected and virus serum titers were determined. The data represent means ± SD among four mice per group.

facilitated Cl-13 infection of high numbers of DCs, which resulted in higher expression levels of negative immune regulators, including interleukin 10 (IL-10) (45), PD-1 (19), T cell immunoglobulin mucin 3 (TIM-3) (46), and lymphocyte activation protein 3 (LAG-3) (47, 48), thus promoting Cl-13 persistence (17, 18, 49). On the other hand, the Q residue at position 1079 within the L polymerase is critical for Cl-13 persistence, and it was associated with robust replication of Cl-13 within DCs (18, 20), but the underlying mechanisms for it remain to be elucidated. In the present work, we have examined the role of residues K465 and G467 within the CD of Cl-13 GP2 in the virus's ability to establish a persistent infection in adult immunocompetent mice. The rationale for these studies stemmed from observations that mutations in the counterpart residues, V459 and K461, of LASV GP2 played a critical role in the early clearance of rCl-13/LASV-GPC in adult immunocompetent B6 mice (26). Our findings have shown that rCl-13 carrying K465V and G467K mutations within the CD of GP2 was unable to persist in mice, which identified these residues as additional viral determinants that play a critical role in the ability of Cl-13 to persist.

Mutations K465V and G467K are located within the CD of GP2 and therefore are highly unlikely to directly affect rCl-13(GPC/VGKS) interaction with αDG, a critical receptor for Cl-13 efficient infection of DCs. However, we cannot rule out the possibility that these mutations could affect, via indirect interactions, the affinity of Cl-13 GP1 for αDG. Residues K465 and G467 are located within the zinc-binding domain (ZBD) in GP2, which is thought to mediate retention of SSP in the GPC complex (50). This GP2-SSP interaction might be affected by mutations K465V and G467K, which could impact virus GPC complex and host cell factor interactions that contribute to the virus's ability to persist *in vivo*.

Our results indicated that the inability of rCl-13(GPC/VGKS) to persist in mice was not due to impaired GPC processing or impaired viral-genome replication and gene transcription. Moreover, rCl-13 WT and rCl-13(GPC/VGKS) exhibited similar fitness in different cell substrates. It is plausible that rCl-13(GPC/VGKS) failed to modulate or abrogate some components of the host early defense responses required to control and clear LCMV. IFN-I sig-

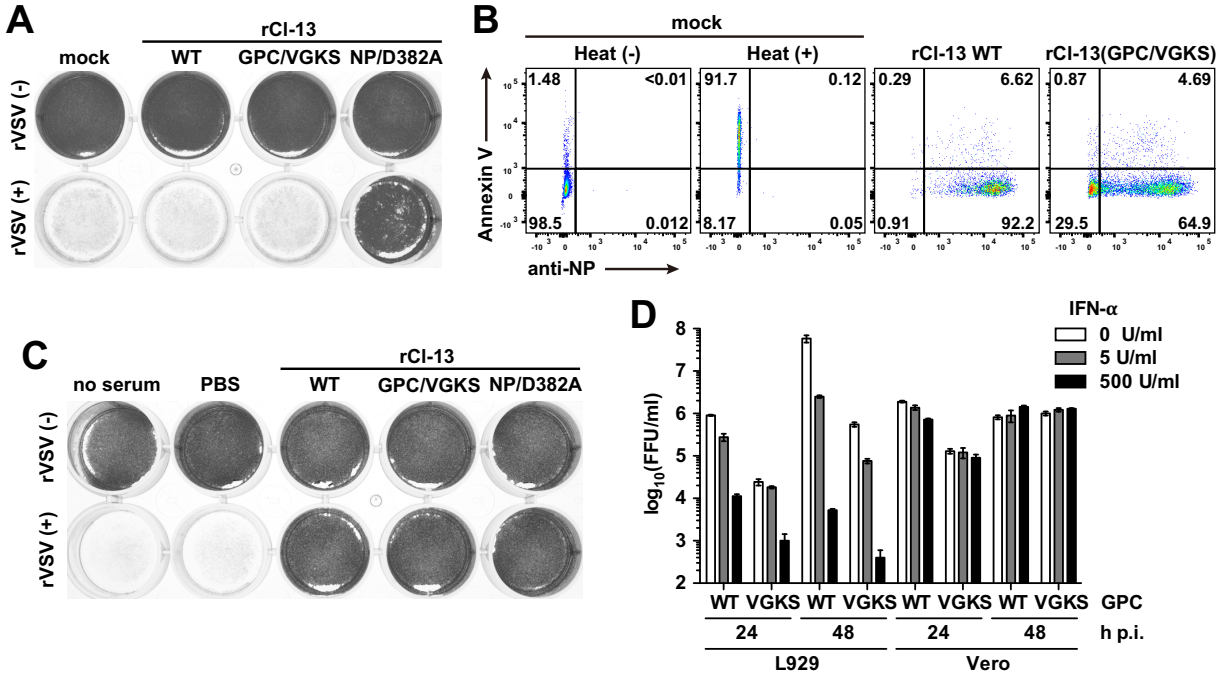

FIG 6 Effects of K465V and G467K mutations on Cl-13's ability to inhibit induction of IFN-I. (A) rCl-13(GPC/VGKS) prevents IFN-I induction. L929 cells seeded in 24-well plates (1.25×10^5 cells/well) and cultured overnight were infected (MOI = 0.1) with rCl-13 WT, rCl-13(GPC/VGKS), or rCl-13(NP/D382A). Twenty-four hours later, LCMV-infected cells were infected with rVSV WT (MOI = 0.01) [rVSV(+)] or remained uninfected [rVSV(−)]. At 36 h p.i. with rVSV, the cells were fixed and stained with crystal violet to assess rVSV-induced CPE. (B) Detection of apoptosis in L929 cells infected with either rCl13 WT or rCl-13(GPC/VGKS). L929 cells (2.5×10^5 cells/well) seeded in a 12-well plate and cultured overnight were infected with either rCl-13 WT or rCl-13(GPC/VGKS) (MOI = 0.1) or remained uninfected (mock). At 48 h p.i., cells were collected. As a positive control, mock-infected cells were incubated at 55°C for 20 min [Heat (+)]. The cells were then stained with fluorescently labeled annexin V and anti-NP antibody (VL-4) and analyzed by flow cytometry. (C) Sera from mice infected with rCl-13(GPC/VGKS) contain levels of bioactive IFN-I that are able to induce the antiviral state in L929 cells and protect against VSV-induced CPE. L929 cells (1.25×10^5 cells/well) seeded in 24-well plates and cultured overnight were treated with sera (1:100 dilution) from mice infected (2×10^6 FFU i.v.) with rCl-13 WT, rCl-13(GPC/VGKS), or rCl-13(NP/D382A) collected at 24 h p.i. After 24 h, the serum-treated cells were infected with rVSV WT (MOI = 0.01) [rVSV (+)] or remained uninfected [rVSV (−)], and at 36 h p.i. with rVSV, the cells were fixed and stained with crystal violet to assess rVSV-induced CPE. (D) K465V and G467K mutations do not affect Cl-13 susceptibility to an IFN-I-induced antiviral state. L929 (1.25×10^5 cells/well) and Vero (1.25×10^5 cells/well) cells were seeded in 24-well plates and cultured overnight, followed by infection (MOI = 0.1) with either rCl-13 WT or rCl-13(GPC/VGKS). After 90 min of virus adsorption, the cells were treated with universal IFN-α at a low (5-U/ml) or high (500-U/ml) concentration or remained untreated. At 24 or 48 h p.i., TCSs were collected and virus titers were determined by an immunofocus assay. The data represent means ± SD of the results of three independent experiments.

naling plays a critical role in Cl-13 persistence, and IFN-I blockade disrupts the establishment of an immune-suppressive milieu characterized by induction of negative immune regulators, disruption of the splenic architecture, and alteration of lymphocyte migration, which result in early clearance of rCl-13 (39). On the other hand, IFN-I signaling triggers the induction of hundreds of interferon-stimulated genes (ISGs) that contribute to the establishment of an antiviral state within cells that inhibits virus multiplication via a plethora of mechanisms. As with many other viruses (51), arenaviruses are also endowed with genes that counteract the host IFN-I response. Thus, both arenavirus NP (52, 53) and Z (54, 55) have been shown to exert a strong inhibitory effect on the induction of IFN-I. rCl-13(GPC/VGKS) encodes WT NP and Z proteins, and as predicted, it was able to efficiently inhibit induction of IFN-I in cultured cells. Notably, many viruses, including LCMV, that efficiently inhibit induction of IFN-I in cultured cells nevertheless trigger a potent host IFN-I response *in vivo*. The contributions of different pattern recognition receptors to LCMV sensing has not been elucidated yet. Likewise, the identities of the specific cell types responsible for the early burst of IFN-I production in LCMV-infected mice have not been unequivocally established, but it appears to involve a complex network of cellular interactions, including pDCs (56, 57). We observed reduced (2-fold) numbers of NP^+ pDCs in mice infected with rCl-13(GPC/VGKS) compared to mice infected with rCl-13, which could have resulted in differences in the host IFN-I response that contributed to the inability of rCl-13(GPC/VGKS) to establish persistence. This scenario seems unlikely, however, as mice infected with either rCl-13 WT or rCl-13(GPC/VGKS) induced similar levels of biologically active IFN-I at early times of infection. We cannot rule out the possibility that in rCl-13(GPC/VGKS)-infected mice, higher (2-fold) numbers of pDCs underwent a nonproductive, or very restricted (NP below detection levels), infection but were still able to trigger production of IFN-I. It is also plausible that biologically active IFN-I at early times of infection was produced by rCl-13(GPC/VGKS)-infected cells other than pDCs. Intriguingly, multiplication of both rCl-13 WT and rCl-13(GPC/VGKS) was similarly inhibited by IFN-α treatment in L929 cells. In contrast, multiplication of both viruses was not significantly affected by treatment with IFN-α in Vero cells, which are unable to produce IFN-I but are fully responsive to treatment with exogenous IFN-I. The reasons for the very different sensitivity of rCl-13(GPC/VGKS), as well as rCl-13 WT, to the IFN-I-induced antiviral state in L929 and Vero cells remain to be deter-

mined. It is plausible that LCMV sensitivity to the IFN-I-induced cell antiviral state is highly dependent on the cell type and species. Together, our results argue against differential susceptibilities between rCl-13 WT and rCl-13(GPC/VGKS) to the IFN-I-induced antiviral state as a contributing factor in the inability of rCl-13(GPC/VGKS) to persist. Likewise, mice infected with either rCl-13 WT or rCl-13(GPC/VGKS) exhibited similar levels of biologically active IFN-I at early times of infection, which has been shown to be required for Cl-13 persistence (39). These results suggest that rCl-13(GPC/VGKS) failed to modulate an as-yet-unidentified immune signaling pathway that is critical for virus persistence.

We did not observe reversions V465K and K467G during serial passages of rCl-13(GPC/VGKS) in cultured cells. In contrast, during replication in IFNAR$^{-/-}$ mice, we observed the selection of revertant K467G. These findings suggest that both K465 and G467 are not strictly required to retain virus fitness, but they are critical for Cl-13 expansion at very early times of infection in the presence of a functional IFN-I system. In addition, G467 seems to be required for long-term robust virus replication in mice independent of the presence or absence of a functional IFN-I system. These results are consistent with previous findings showing that rCl-13/LASV-GPC with a single G461 mutation was able to persist in mice for up to 2 weeks, whereas rCl-13/LASV-GPC carrying both K459 and G461 further enhanced viral replication in mice (26). Future studies aimed at phenotypically characterizing rCl-13 with either V465 or K467 mutations will contribute to a better understanding of the roles played by the CD of GP2 in arenavirus persistence.

Cl-13 infects a larger number of pDCs than ARM (20, 38, 39), which results in the establishment of an immune environment beneficial for virus persistence, including disruption of DC function (22), disorganization of the splenic architecture (58, 59), and robust expression of negative immune regulators (19, 45, 46, 60, 61). Consistent with these findings, K465V and G467K mutations within the CD of GP2 of the nonpersistent rCl-13(GPC/VGKS) were associated with reduced numbers of Cl-13-infected pDCs compared to rCl-13 WT. Reduced numbers of NP$^+$ pDCs in mice infected with rCl-13(GPC/VGKS) could reflect the fact that rCl-13(GPC/VGKS) replicates less efficiently than rCl-13 WT in pDCs. However, this seems unlikely, because rCl-13(GPC/VGKS) has the Q1079 mutation within the L polymerase, which has been shown to increase replication in DCs and to provide robust replication in cell-based assays (18, 20). Alternatively, the K465V and G467K mutations may interfere with virus cell entry, despite these mutations being located within the CD of GP2. Interestingly, human pDCs are refractory to rCl-13 WT infection when infected *ex vivo* (62), suggesting the existence of a yet-unidentified cell entry pathway required for infection of pDCs *in vivo* that could be affected by K465V and G467K mutations. Published data support a very strong correlation between high affinity for αDG of the LCMV GP and the virus's ability to persist. However, the role of αDG in Cl-13 infection of pDCs has not been entirely elucidated. We have shown that human pDCs are refractory *ex vivo* to infection with Cl-13. Accordingly, human pDCs did not produce IFN-I in response to infection with cell-free Cl-13, but they produced high levels of IFN-I following cell-cell contact with Cl-13-infected cells (62). Thus, infection of pDCs *in vivo* might require direct contact with other LCMV-infected cells. It is plausible that rCl-13(GPC/VGKS) inefficiently infects cells required for infection of pDCs through cell-cell contact, which resulted in reduced numbers of NP$^+$ pDCs in mice infected with rCl-13(GPC/VGKS). This, in turn, prevented the establishment of persistence by rCl-13(GPC/VGKS).

ACKNOWLEDGMENTS

We thank B. Ware for his help with collecting and analyzing the flow cytometry data for the detection of apoptotic cells.

This research was supported by NIH/NIAID grants AI047140 and AI077719 to J.C.D.L.T. and by Japan Society for the Promotion of Science, Daiichi Sankyo Foundation of Life Science, and KANAE Foundation for the Promotion of Medical Science grants to M.I.

FUNDING INFORMATION

This work, including the efforts of Masaharu Iwasaki, was funded by KANAE Foundation for the Promotion of Medical Science. This work, including the efforts of Juan Carlos de la Torre, was funded by HHS | NIH | National Institute of Allergy and Infectious Diseases (NIAID) (AI047140 and AI077719). This work, including the efforts of Masaharu Iwasaki, was funded by Japan Society for the Promotion of Science (JSPS). This work, including the efforts of Masaharu Iwasaki, was funded by Daiichi Sankyo Foundation of Life Science.

REFERENCES

1. **Buchmeier MJ, Peters CJ, de la Torre JC.** 2007. Arenaviridae: the viruses and their replication, p 1791–1851. *In* Knipe DM, Howley PM, Griffin DE, Lamb RA, Martin MA, Roizman B, Straus SE (ed), Fields virology, 5th ed, vol 2. Lippincott Williams & Wilkins, Philadelphia, PA.
2. **Perez M, Craven RC, de la Torre JC.** 2003. The small RING finger protein Z drives arenavirus budding: implications for antiviral strategies. Proc Natl Acad Sci U S A **100:**12978–12983. http://dx.doi.org/10.1073/pnas.2133782100.
3. **Strecker T, Eichler R, Meulen J, Weissenhorn W, Dieter Klenk H, Garten W, Lenz O.** 2003. Lassa virus Z protein is a matrix protein and sufficient for the release of virus-like particles. J Virol **77:**10700–10705. http://dx.doi.org/10.1128/JVI.77.19.10700-10705.2003.
4. **Bray M.** 2005. Pathogenesis of viral hemorrhagic fever. Curr Opin Immunol **17:**399–403. http://dx.doi.org/10.1016/j.coi.2005.05.001.
5. **Geisbert TW, Jahrling PB.** 2004. Exotic emerging viral diseases: progress and challenges. Nat Med **10:**S110–S121. http://dx.doi.org/10.1038/nm1142.
6. **Richmond JK, Baglole DJ.** 2003. Lassa fever: epidemiology, clinical features, and social consequences. BMJ **327:**1271–1275. http://dx.doi.org/10.1136/bmj.327.7426.1271.
7. **Freedman DO, Woodall J.** 1999. Emerging infectious diseases and risk to the traveler. Med Clin North Am **83:**865–883, v.
8. **Isaacson M.** 2001. Viral hemorrhagic fever hazards for travelers in Africa. Clin Infect Dis **33:**1707–1712. http://dx.doi.org/10.1086/322620.
9. **Briese T, Paweska JT, McMullan LK, Hutchison SK, Street C, Palacios G, Khristova ML, Weyer J, Swanepoel R, Egholm M, Nichol ST, Lipkin WI.** 2009. Genetic detection and characterization of Lujo virus, a new hemorrhagic fever-associated arenavirus from southern Africa. PLoS Pathog **5:**e1000455. http://dx.doi.org/10.1371/journal.ppat.1000455.
10. **Paweska JT, Sewlall NH, Ksiazek TG, Blumberg LH, Hale MJ, Lipkin WI, Weyer J, Nichol ST, Rollin PE, McMullan LK, Paddock CD, Briese T, Mnyaluza J, Dinh TH, Mukonka V, Ching P, Duse A, Richards G, de Jong G, Cohen C, Ikalafeng B, Mugero C, Asomugha C, Malotle MM, Nteo DM, Misiani E, Swanepoel R, Zaki SR, Outbreak Control and Investigation Teams.** 2009. Nosocomial outbreak of novel arenavirus infection, southern Africa. Emerg Infect Dis **15:**1598–1602. http://dx.doi.org/10.3201/eid1510.090211.
11. **Olschlager S, Flatz L.** 2013. Vaccination strategies against highly pathogenic arenaviruses: the next steps toward clinical trials. PLoS Pathog **9:**e1003212. http://dx.doi.org/10.1371/journal.ppat.1003212.
12. **Bausch DG, Hadi CM, Khan SH, Lertora JJ.** 2010. Review of the literature and proposed guidelines for the use of oral ribavirin as postexposure prophylaxis for Lassa fever. Clin Infect Dis **51:**1435–1441. http://dx.doi.org/10.1086/657315.
13. **Damonte EB, Coto CE.** 2002. Treatment of arenavirus infections: from

basic studies to the challenge of antiviral therapy. Adv Virus Res **58:**125–155. http://dx.doi.org/10.1016/S0065-3527(02)58004-0.
14. **Hadi CM, Goba A, Khan SH, Bangura J, Sankoh M, Koroma S, Juana B, Bah A, Coulibaly M, Bausch DG.** 2010. Ribavirin for Lassa fever postexposure prophylaxis. Emerg Infect Dis **16:**2009–2011. http://dx.doi.org/10.3201/eid1612.100994.
15. **McCormick JB, Fisher-Hoch SP.** 2002. Lassa fever. Curr Top Microbiol Immunol **262:**75–109.
16. **Ahmed R, Salmi A, Butler LD, Chiller JM, Oldstone MB.** 1984. Selection of genetic variants of lymphocytic choriomeningitis virus in spleens of persistently infected mice. Role in suppression of cytotoxic T lymphocyte response and viral persistence. J Exp Med **160:**521–540.
17. **Salvato M, Borrow P, Shimomaye E, Oldstone MB.** 1991. Molecular basis of viral persistence: a single amino acid change in the glycoprotein of lymphocytic choriomeningitis virus is associated with suppression of the antiviral cytotoxic T-lymphocyte response and establishment of persistence. J Virol **65:**1863–1869.
18. **Sullivan BM, Emonet SF, Welch MJ, Lee AM, Campbell KP, de la Torre JC, Oldstone MB.** 2011. Point mutation in the glycoprotein of lymphocytic choriomeningitis virus is necessary for receptor binding, dendritic cell infection, and long-term persistence. Proc Natl Acad Sci U S A **108:**2969–2974. http://dx.doi.org/10.1073/pnas.1019304108.
19. **Barber DL, Wherry EJ, Masopust D, Zhu B, Allison JP, Sharpe AH, Freeman GJ, Ahmed R.** 2006. Restoring function in exhausted CD8 T cells during chronic viral infection. Nature **439:**682–687. http://dx.doi.org/10.1038/nature04444.
20. **Bergthaler A, Flatz L, Hegazy AN, Johnson S, Horvath E, Lohning M, Pinschewer DD.** 2010. Viral replicative capacity is the primary determinant of lymphocytic choriomeningitis virus persistence and immunosuppression. Proc Natl Acad Sci U S A **107:**21641–21646. http://dx.doi.org/10.1073/pnas.1011998107.
21. **Sevilla N, Kunz S, Holz A, Lewicki H, Homann D, Yamada H, Campbell KP, de La Torre JC, Oldstone MB.** 2000. Immunosuppression and resultant viral persistence by specific viral targeting of dendritic cells. J Exp Med **192:**1249–1260. http://dx.doi.org/10.1084/jem.192.9.1249.
22. **Sevilla N, McGavern DB, Teng C, Kunz S, Oldstone MB.** 2004. Viral targeting of hematopoietic progenitors and inhibition of DC maturation as a dual strategy for immune subversion. J Clin Invest **113:**737–745. http://dx.doi.org/10.1172/JCI20243.
23. **Kunz S, Sevilla N, McGavern DB, Campbell KP, Oldstone MB.** 2001. Molecular analysis of the interaction of LCMV with its cellular receptor [alpha]-dystroglycan. J Cell Biol **155:**301–310. http://dx.doi.org/10.1083/jcb.200104103.
24. **Zhang C, Hu B, Xiao L, Liu Y, Wang P.** 2014. Pseudotyping lentiviral vectors with lymphocytic choriomeningitis virus glycoproteins for transduction of dendritic cells and in vivo immunization. Hum Gene Ther Methods **25:**328–338. http://dx.doi.org/10.1089/hgtb.2014.105.
25. **Lee AM, Cruite J, Welch MJ, Sullivan B, Oldstone MB.** 2013. Pathogenesis of Lassa fever virus infection. I. Susceptibility of mice to recombinant Lassa Gp/LCMV chimeric virus. Virology **442:**114–121. http://dx.doi.org/10.1016/j.virol.2013.04.010.
26. **Sommerstein R, Ramos da Palma J, Olschlager S, Bergthaler A, Barba L, Lee BP, Pasquato A, Flatz L.** 2014. Evolution of recombinant lymphocytic choriomeningitis virus/Lassa virus in vivo highlights the importance of the GPC cytosolic tail in viral fitness. J Virol **88:**8340–8348. http://dx.doi.org/10.1128/JVI.00236-14.
27. **Lee KJ, Novella IS, Teng MN, Oldstone MB, de La Torre JC.** 2000. NP and L proteins of lymphocytic choriomeningitis virus (LCMV) are sufficient for efficient transcription and replication of LCMV genomic RNA analogs. J Virol **74:**3470–3477. http://dx.doi.org/10.1128/JVI.74.8.3470-3477.2000.
28. **Lee KJ, Perez M, Pinschewer DD, de la Torre JC.** 2002. Identification of the lymphocytic choriomeningitis virus (LCMV) proteins required to rescue LCMV RNA analogs into LCMV-like particles. J Virol **76:**6393–6397. http://dx.doi.org/10.1128/JVI.76.12.6393-6397.2002.
29. **Rodrigo WW, de la Torre JC, Martinez-Sobrido L.** 2011. Use of single-cycle infectious lymphocytic choriomeningitis virus to study hemorrhagic fever arenaviruses. J Virol **85:**1684–1695. http://dx.doi.org/10.1128/JVI.02229-10.
30. **Emonet SF, Garidou L, McGavern DB, de la Torre JC.** 2009. Generation of recombinant lymphocytic choriomeningitis viruses with trisegmented genomes stably expressing two additional genes of interest. Proc Natl Acad Sci U S A **106:**3473–3478. http://dx.doi.org/10.1073/pnas.0900088106.
31. **Flatz L, Bergthaler A, de la Torre JC, Pinschewer DD.** 2006. Recovery of an arenavirus entirely from RNA polymerase I/II-driven cDNA. Proc Natl Acad Sci U S A **103:**4663–4668. http://dx.doi.org/10.1073/pnas.0600652103.
32. **Sanchez AB, de la Torre JC.** 2006. Rescue of the prototypic Arenavirus LCMV entirely from plasmid. Virology **350:**370–380. http://dx.doi.org/10.1016/j.virol.2006.01.012.
33. **Battegay M.** 1993. Quantification of lymphocytic choriomeningitis virus with an immunological focus assay in 24 well plates. ALTEX **10:**6–14.
34. **Rojek JM, Kunz S.** 2008. Cell entry by human pathogenic arenaviruses. Cell Microbiol **10:**828–835. http://dx.doi.org/10.1111/j.1462-5822.2007.01113.x.
35. **Kunz S, Edelmann KH, de la Torre JC, Gorney R, Oldstone MB.** 2003. Mechanisms for lymphocytic choriomeningitis virus glycoprotein cleavage, transport, and incorporation into virions. Virology **314:**168–178. http://dx.doi.org/10.1016/S0042-6822(03)00421-5.
36. **Schlie K, Strecker T, Garten W.** 2010. Maturation cleavage within the ectodomain of Lassa virus glycoprotein relies on stabilization by the cytoplasmic tail. FEBS Lett **584:**4379–4382. http://dx.doi.org/10.1016/j.febslet.2010.09.032.
37. **Sullivan BM, Teijaro JR, de la Torre JC, Oldstone MB.** 2015. Early virus-host interactions dictate the course of a persistent infection. PLoS Pathog **11:**e1004588. http://dx.doi.org/10.1371/journal.ppat.1004588.
38. **Macal M, Lewis GM, Kunz S, Flavell R, Harker JA, Zuniga EI.** 2012. Plasmacytoid dendritic cells are productively infected and activated through TLR-7 early after arenavirus infection. Cell Host Microbe **11:**617–630. http://dx.doi.org/10.1016/j.chom.2012.04.017.
39. **Teijaro JR, Ng C, Lee AM, Sullivan BM, Sheehan KC, Welch M, Schreiber RD, de la Torre JC, Oldstone MB.** 2013. Persistent LCMV infection is controlled by blockade of type I interferon signaling. Science **340:**207–211. http://dx.doi.org/10.1126/science.1235214.
40. **Sevilla N, Kunz S, McGavern D, Oldstone MB.** 2003. Infection of dendritic cells by lymphocytic choriomeningitis virus. Curr Top Microbiol Immunol **276:**125–144.
41. **Wang Y, Swiecki M, Cella M, Alber G, Schreiber RD, Gilfillan S, Colonna M.** 2012. Timing and magnitude of type I interferon responses by distinct sensors impact CD8 T cell exhaustion and chronic viral infection. Cell Host Microbe **11:**631–642. http://dx.doi.org/10.1016/j.chom.2012.05.003.
42. **Martinez-Sobrido L, Emonet S, Giannakas P, Cubitt B, Garcia-Sastre A, de la Torre JC.** 2009. Identification of amino acid residues critical for the anti-interferon activity of the nucleoprotein of the prototypic arenavirus lymphocytic choriomeningitis virus. J Virol **83:**11330–11340. http://dx.doi.org/10.1128/JVI.00763-09.
43. **Iwasaki M, Cubitt B, Sullivan BM, de la Torre JC.** 2016. The high degree of sequence plasticity of the arenavirus noncoding intergenic region (IGR) enables the use of a nonviral universal synthetic IGR to attenuate arenaviruses. J Virol **90:**3187–3197. http://dx.doi.org/10.1128/JVI.03145-15.
44. **Kunz S, Rojek JM, Perez M, Spiropoulou CF, Oldstone MB.** 2005. Characterization of the interaction of Lassa fever virus with its cellular receptor alpha-dystroglycan. J Virol **79:**5979–5987. http://dx.doi.org/10.1128/JVI.79.10.5979-5987.2005.
45. **Brooks DG, Trifilo MJ, Edelmann KH, Teyton L, McGavern DB, Oldstone MB.** 2006. Interleukin-10 determines viral clearance or persistence in vivo. Nat Med **12:**1301–1309. http://dx.doi.org/10.1038/nm1492.
46. **Jin HT, Anderson AC, Tan WG, West EE, Ha SJ, Araki K, Freeman GJ, Kuchroo VK, Ahmed R.** 2010. Cooperation of Tim-3 and PD-1 in CD8 T-cell exhaustion during chronic viral infection. Proc Natl Acad Sci U S A **107:**14733–14738. http://dx.doi.org/10.1073/pnas.1009731107.
47. **Blackburn SD, Shin H, Freeman GJ, Wherry EJ.** 2008. Selective expansion of a subset of exhausted CD8 T cells by alphaPD-L1 blockade. Proc Natl Acad Sci U S A **105:**15016–15021. http://dx.doi.org/10.1073/pnas.0801497105.
48. **Richter K, Agnellini P, Oxenius A.** 2010. On the role of the inhibitory receptor LAG-3 in acute and chronic LCMV infection. Int Immunol **22:**13–23. http://dx.doi.org/10.1093/intimm/dxp107.
49. **Matloubian M, Somasundaram T, Kolhekar SR, Selvakumar R, Ahmed R.** 1990. Genetic basis of viral persistence: single amino acid change in the viral glycoprotein affects ability of lymphocytic choriomeningitis virus to persist in adult mice. J Exp Med **172:**1043–1048. http://dx.doi.org/10.1084/jem.172.4.1043.
50. **Briknarova K, Thomas CJ, York J, Nunberg JH.** 2011. Structure of a

zinc-binding domain in the Junin virus envelope glycoprotein. J Biol Chem **286:**1528–1536. http://dx.doi.org/10.1074/jbc.M110.166025.

51. **Versteeg GA, Garcia-Sastre A.** 2010. Viral tricks to grid-lock the type I interferon system. Curr Opin Microbiol **13:**508–516. http://dx.doi.org/10.1016/j.mib.2010.05.009.
52. **Martinez-Sobrido L, Zuniga EI, Rosario D, Garcia-Sastre A, de la Torre JC.** 2006. Inhibition of the type I interferon response by the nucleoprotein of the prototypic arenavirus lymphocytic choriomeningitis virus. J Virol **80:**9192–9199. http://dx.doi.org/10.1128/JVI.00555-06.
53. **Rodrigo WW, Ortiz-Riano E, Pythoud C, Kunz S, de la Torre JC, Martinez-Sobrido L.** 2012. Arenavirus nucleoproteins prevent activation of nuclear factor kappa B. J Virol **86:**8185–8197. http://dx.doi.org/10.1128/JVI.07240-11.
54. **Fan L, Briese T, Lipkin WI.** 2010. Z proteins of New World arenaviruses bind RIG-I and interfere with type I interferon induction. J Virol **84:**1785–1791. http://dx.doi.org/10.1128/JVI.01362-09.
55. **Xing J, Ly H, Liang Y.** 2015. The Z proteins of pathogenic but not nonpathogenic arenaviruses inhibit RIG-I-like receptor-dependent interferon production. J Virol **89:**2944–2955. http://dx.doi.org/10.1128/JVI.03349-14.
56. **Jung A, Kato H, Kumagai Y, Kumar H, Kawai T, Takeuchi O, Akira S.** 2008. Lymphocytoid choriomeningitis virus activates plasmacytoid dendritic cells and induces a cytotoxic T-cell response via MyD88. J Virol **82:**196–206. http://dx.doi.org/10.1128/JVI.01640-07.
57. **Montoya M, Edwards MJ, Reid DM, Borrow P.** 2005. Rapid activation of spleen dendritic cell subsets following lymphocytic choriomeningitis virus infection of mice: analysis of the involvement of type 1 IFN. J Immunol **174:**1851–1861. http://dx.doi.org/10.4049/jimmunol.174.4.1851.
58. **Muller S, Hunziker L, Enzler S, Buhler-Jungo M, Di Santo JP, Zinkernagel RM, Mueller C.** 2002. Role of an intact splenic microarchitecture in early lymphocytic choriomeningitis virus production. J Virol **76:**2375–2383. http://dx.doi.org/10.1128/jvi.76.5.2375-2383.2002.
59. **Odermatt B, Eppler M, Leist TP, Hengartner H, Zinkernagel RM.** 1991. Virus-triggered acquired immunodeficiency by cytotoxic T-cell-dependent destruction of antigen-presenting cells and lymph follicle structure. Proc Natl Acad Sci U S A **88:**8252–8256. http://dx.doi.org/10.1073/pnas.88.18.8252.
60. **Ejrnaes M, Filippi CM, Martinic MM, Ling EM, Togher LM, Crotty S, von Herrath MG.** 2006. Resolution of a chronic viral infection after interleukin-10 receptor blockade. J Exp Med **203:**2461–2472. http://dx.doi.org/10.1084/jem.20061462.
61. **Ng CT, Oldstone MB.** 2012. Infected CD8alpha$^-$ dendritic cells are the predominant source of IL-10 during establishment of persistent viral infection. Proc Natl Acad Sci U S A **109:**14116–14121. http://dx.doi.org/10.1073/pnas.1211910109.
62. **Wieland SF, Takahashi K, Boyd B, Whitten-Bauer C, Ngo N, de la Torre JC, Chisari FV.** 2014. Human plasmacytoid dendritic cells sense lymphocytic choriomeningitis virus-infected cells in vitro. J Virol **88:**752–757. http://dx.doi.org/10.1128/JVI.01714-13.